

Multiscale physics of ion-induced radiation damage

Eugene Surdutovich^{1, 2} and Andrey V. Solov'yov^{2,3}

¹ Department of Physics, Oakland University, Rochester, Michigan 48309, USA

² Frankfurt Institute for Advanced Studies, Ruth-Moufang-Str. 1, 60438 Frankfurt am Main, Germany

E-mail: surdutov@oakland.edu

Abstract. A multiscale approach to the physics of ion-beam cancer therapy, an approach suggested in order to understand the interplay of a large number of phenomena involved in radiation damage scenario occurring on a range of temporal, spatial, and energy scales, is being reviewed. The scenario is described along with a variety of effects that take place on different temporal, spatial, and energy scales and play major roles in the scenario of interaction of ions with tissue. The understanding of these effects leads to a quantitative assessment of relative biological effectiveness that relates the physical quantities, such as dose, to the biological values, such as the probability of cell survival.

1. Introduction

The development of ion-beam cancer therapy (IBCT) and other applications of ions boosted the scientific interest in obtaining of deeper understanding of radiation damage with ions. A number of important scientific questions related to the assessment of biological damage on the molecular level, have not yet been resolved. Therefore, this field has attracted much attention from the scientific community [1, 2, 3, 4, 5]. The COST ⁴ Action, “Nano-scale insights in ion beam cancer therapy (Nano-IBCT)” [6], approved in 2010, opened an opportunity for a wide exchange between scientists in different areas specifically devoted to the fundamental studies related to IBCT. Among these studies is the multiscale approach to the assessment of radiation damage induced by irradiation with ions. It is aimed at a phenomenon-based quantitative understanding of the scenario from the incidence of an energetic ion on tissue to the cell death. This method combines many spatial, temporal, and energy scales, and is therefore a truly multiscale approach.

The multiscale approach was formulated in Refs. [5, 7], where a scenario leading to DNA damage was suggested. Then, it was elaborated upon as different aspects of the scenario were added in a series of works [8, 9, 10, 11, 12, 13, 14, 15]. Its name emphasizes the fact that important interactions involved in the scenario happen on a variety of temporal, spatial, and energy scales. Right from the beginning, the approach was formulated as phenomenon-based and was aimed at elucidating the physical, chemical, or biological effects that are important or dominating on each scale in time, space, and energy.

The multiscale approach raised questions about the nature of the effects that define the biological outcome and predict the relative biological effectiveness (RBE) [1, 2] and explain

³ On leave from A.F. Ioffe Physical Technical Institute, St. Petersburg, Russia.

⁴ European framework for Cooperation in Science and Technology



the survival curves that relate the dose with the probability of cell survival. The main issues addressed by the multiscale approach are ion stopping in the medium, the production and transport of secondary electrons produced as a result of ionization and excitation of the medium, the interaction of secondary particles with biological molecules, the most important being DNA, the analysis of induced damage, and the evaluation of the probabilities of subsequent cell survival or death. These effects are happening on time scales ranging from 10^{-21} to 10^{-5} s, i.e., from nuclear to biochemical times. The aim of the physical part of the analysis is the calculation of the spatial distribution of primary DNA damage, including the degree of complexity of this damage.

The scenario of the radiation damage is described in Section 2, then the key effects on consequent time scales are reviewed in Sections 3-5.

2. Multiscale scenario of radiation damage

Radiation damage due to ionizing radiation is initiated by the projectiles incident on tissue. Initially they have energy ranging from a few to hundreds of MeV. In the process of propagation through tissue they transfer their energy in the processes of ionization, excitation, nuclear fragmentation, etc. Naturally, the radiation damage is associated with the transferred energy, and the dose (i.e., absorbed energy density) is a common indicator for the assessment of the damage [1, 2]. In the case of ion therapy, the profile of dose deposition along the ion's path is characterised with a plateau followed by a sharp Bragg peak. The position of this peak depends on the initial energy of the ion and marks the location of the maximum radiation damage. In the process of radiation therapy, a tumour is being "scanned" with the Bragg peak in order to deposit a large dose to the target and spare healthy tissues surrounding it.

However, the deposition of large doses in the vicinity of the Bragg peak does not explain how the radiation damage occurs, since projectiles themselves only interact with a few biomolecules on their way and this direct damage is only a small fraction of overall damage. It is commonly understood that the secondary electrons produced in the process of ionization of the medium with ions are largely responsible for the vast portion of biodamage. Let us discuss the scenario which explains it.

Secondary electrons are produced during a rather short time of $10^{-18} - 10^{-17}$ s following the ion's passage. These energy spectrum of these electrons has extensively been discussed in the literature [16, 17, 18, 8, 9] and the main result (relevant for this discussion) is that the most secondary electrons have energy below 50 eV and only a few (referred to as δ -electrons) have high (> 100 eV) energy. Moreover, this is true for a very large range of ion's energy. This has several important consequences. First, the ranges of propagation of these electrons in tissue are rather small, around 3 nm. Second, the angular distribution is largely uniform [19]; this allows one to consider their transport using random walk approach [5, 12, 20, 21, 22].

The next time scale $10^{-16} - 10^{-15}$ s corresponds to the propagation of secondary electrons in tissue. These electrons (which start with about 45-50 eV energy) are called ballistic. Their initial mean elastic and ionization free paths (in liquid water) are about 0.43 and 3.5 nm, respectively. This means that they ionize a molecule after about seven elastic collisions, while the probability of second ionization is small [8]. Thus the secondary electrons are losing their energy. This happens within 1-1.5 nm of the ion's path. After that they continue propagating elastically scattering with the molecules of the medium until they get bound or solvated electrons are formed. It is important to notice, that these low energy electrons remain important agents for biodamage since they can attach to biomolecules like DNA causing dissociation [23, 24]. The solvated electrons may play the main role in the damage scenario as well [25].

Yet, the energy lost by electrons during the previous stage is transferred to the medium, and as a result of this transfer, the medium becomes very hot [10]. This happens within about 1 – 1.5-nm cylinder around the ion's path, which we refer to as the hot cylinder. The pressure

inside this cylinder increases by a factor of about 10^3 compared to the atmospheric pressure in the medium outside the cylinder. This pressure builds up by about $10^{-14} - 10^{-13}$ s and it is a source of a cylindrical shock wave [11]. This shock wave propagates through in medium for about $10^{-13} - 10^{-11}$ s. Its relevance to the biodamage is as follows. If the shock wave is strong enough (the strength depends on the distance from the ion's path and the LET), it may inflict damage directly by breaking covalent bonds in a DNA molecule [14]. Besides, the radial collective motion that takes place during this time is instrumental in propagating the highly reactive species such as hydroxyl radicals, just formed solvated electrons, etc. to a larger distances (up to tens of nm) thus increasing the area of an ion's impact.

We assess the primary damage to DNA molecules and other parts of cells due to the above effects. This damage happens during the following 10^{-5} s and consists of various lesions on DNA and other biomolecules. Some of these lesions may be repaired by the living system, but some may not and the latter may lead to the cell death. The whole scenario is shown in Figure 1.

3. Ion stopping and the Bragg peak

The scenario starts with the ion's propagation in a medium. The Bragg peak in the stopping power of massive charged particles is obtained using a version of the Bethe - Bloch formula [26, 27, 28]. This formula provides the dependence of the stopping power on the energy of the ion and practically depends on the mean excitation energy. In the majority of works, liquid water was used as a tissue substitute because human cells on the average consist of 75% water. This energy for liquid water is chosen somewhere between 70 and 80 eV [29, 30]. Our approach to this problem was different; we used the singly-differentiated (with respect to the secondary electron energy) ionization cross sections of water molecules in the medium as a physical input [8, 9]. These cross sections were taken from experiments [31] with parameters tuned for liquid water [9]. The parameterizations were also modified to take into account relativistic effects in the beginning of the ion's path. Even a slight change in cross sections in the entrance channel (plateau region of LET curve) may significantly affect the position of the Bragg peak. Energy loss due to excitation of water molecules has also been included in the calculations [8]. The effect of charge transfer strongly affects the height of the Bragg peak, since it is proportional to the square of the effective charge of the projectile and the latter decreases as the projectile slows down because of the pick off electrons. Barkas's parameterization [32] was used for the calculation of the effective charge. The next effect, included in Ref. [8], was the scattering of projectiles that naturally occurs as they propagate in the medium. This causes the spread in longitudinal velocities or the so-called energy straggling. This widens and substantially diminishes the Bragg peak for the beam of projectiles. Another effect on this scale, not yet included in the multiscale approach, is the nuclear fragmentation that happens quite often when projectiles collide with the nuclei of the medium. This effect is deemed to be significant, especially for the calculations of the tail in the stopping power curve beyond the Bragg peak [30]. As a consequence, we were able to describe the Bragg peak in good agreement with simulations and experiments [8, 9, 33].

An important difference of our approach, relying on the singly-differentiated ionization cross section, allowed us to not only describe the Bragg peak, but also to use these cross sections to calculate the energy spectrum of secondary electrons, which turned out to be quite useful on the following scale of the electron transport and interactions of electrons with the medium.

A new development has been reported in Ref. [15], where a semiempirical model for calculating the electron emission from any organic compound after ion impact was employed in order to extend the calculations to a more realistic medium than liquid water. With the only input of density and composition of the target a quite accurate evaluation of ionization cross sections for such media became possible. Results for protons impacting in the most representative biological targets, such as water or DNA components, showed a good comparison with experimental data.

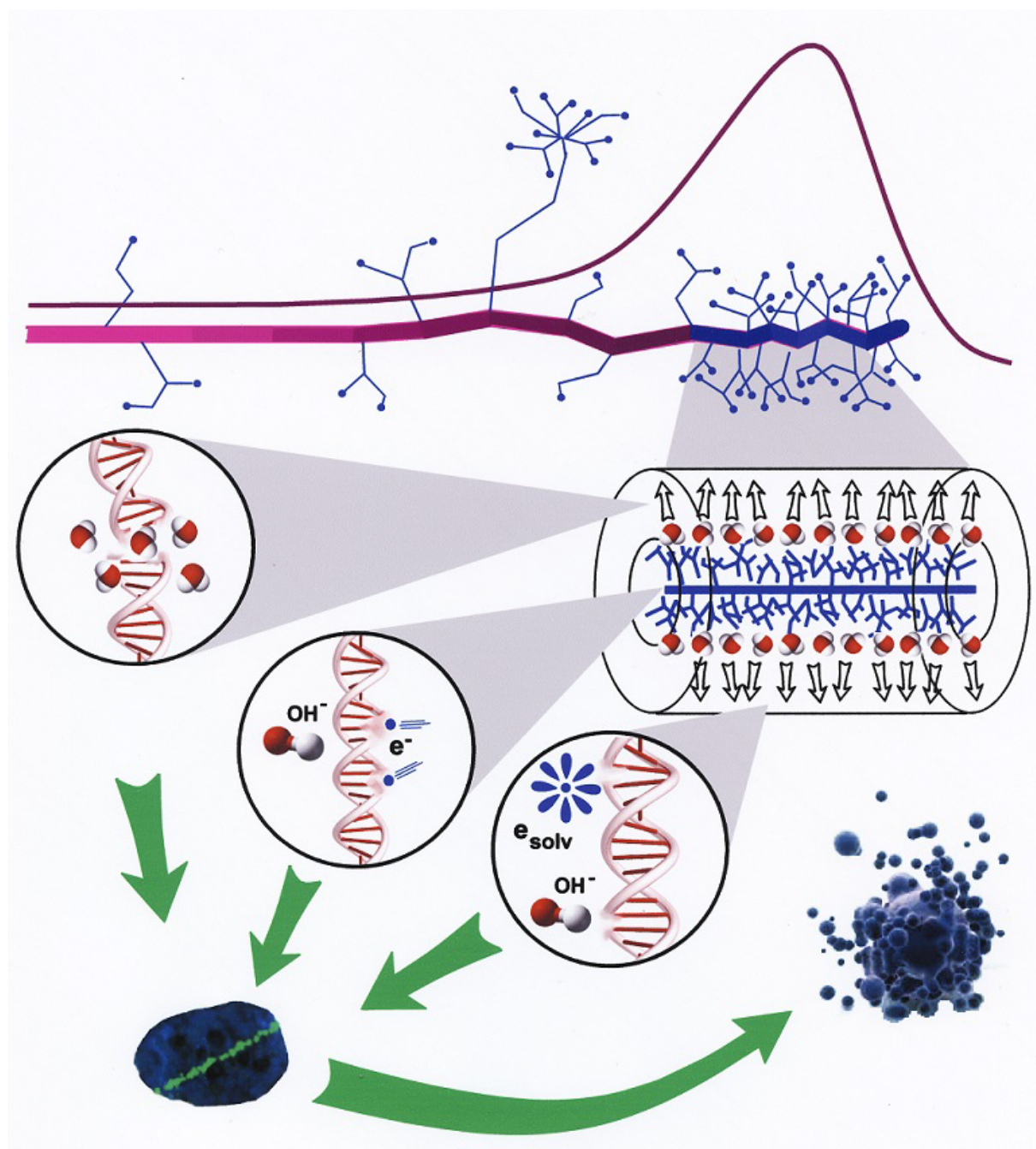


Figure 1. The scenario of biological damage with ions. Ion propagation is shown on top along with production of secondary electrons and the Bragg peak. Then the Bragg peak area is zoomed up to show propagation of secondary electrons within the hot cylinder and then a shock wave in liquid water expanding to the size of large cylinder. Three mechanisms of DNA damage are shown: with energetic water molecules of the shock wave, with ballistic electrons and radicals inside the hot cylinder, and with radicals and solvated electrons at the surface of the large cylinder. The next stage of biological repair is shown as repair protein foci on the background of the cell nucleus. Finally, the last stage is an apoptotic cell, representing a probable cell death.

Due to its simplicity and great predictive effectiveness, the method can be immediately extended to any combination of biological target and charged particle of interest in ion beam cancer therapy. As a result, the Bragg peak as well as the energy spectra of secondary electrons can be calculated for more complicated media than liquid water.

4. Transport of secondary electrons and DNA damage

The next scale in energy and space is related to the transport of the secondary particles, which has been considered in Refs. [5, 34, 12, 22]. These papers were built on the inference from the analysis of the energy distribution of secondary electrons that the average energy of these electrons is about 45-50 eV. At these and lower energies, the ionization cross sections are nearly isotropic, which allows one to employ a random walk approximation, i.e., assume that most of secondary electrons (excluding the more energetic δ -electrons) diffuse out from the ion's path. This diffusion was explored in a series of problems. First, we considered a random walk of electrons from the ion's path to a twist of DNA located at some distance from the path [5]. A single twist of a DNA molecule was chosen because it is an important unit for investigations of double strand breaks (DSBs), significant for the assessment of cell survival. In that study, the number of DSBs per μm of ion's path due to secondary electron action was estimated and compared with biophysical experiments [35].

A later development of that work in Ref. [12] explored a random walk approximation in order to assess the complex DNA damage. Complex DNA damage, investigated by biologists in Refs. [36, 37, 38, 39], is defined as a multiple number of primary DNA lesions happening on a length of two DNA twists. Such a correlation of lesions is called a cluster with a size equal to the number of singly-damaged sites. Different types of lesions may be qualified as effective, e.g., single strand breaks (SSBs), DSBs, base-damages, abasic sites, etc. The size of a cluster is related to the probability of its enzymatic repair. It is deemed that clusters of a sufficiently large size (larger than three or four lesions) are lethal for the cell. Thus, the problem of assessment of complex damage can, on the one hand, be tackled in the same fashion as the problem of DSB, described above; on the other hand, its solution is directly related to the assessment of cell survival as a result of irradiation with ions. The target for a complex damage site is a two-twist segment of a DNA molecule. The original idea for the calculation of complex damage was formulated in Ref. [40]. There, it was suggested that each lesion that counts in a cluster is due to an action of a single agent such as a secondary electron, a radical, etc. Then, if the average number of lesions per target N_i is calculated, the probability of occurrences of clusters of different size, $P_\nu(N_i)$, can be calculated using a Poisson distribution,

$$P_\nu = \exp(-N_i) \frac{N_i^\nu}{\nu!}, \quad (1)$$

where ν is the degree of complexity [40, 12]. The calculation of N_i , were solved using the random walk approach [21]. In that recent work, the random walk calculations of the fluence were successfully compared with the Monte Carlo simulation of transport of secondary electrons.

The radial distribution of clustered damage sites can be obtained using Eq. (1) and the radial dependence of N_i . Given that damage clusters with degree of complexity exceeding a certain number are lethal (this information comes from the biologists [39]), we can obtain the radial distribution of cell survival. Independently, the radial dose distribution around the ion's path can also be calculated using the random walk approach [20]. Then, the survival curve can be obtained as a parametric plot of cell survival on the radial dose [12].

This is an example of how the multiscale approach can be used for assessment of radiation damage. The involved quantities, the cell survival and the radial dose, are calculated independently based on either physical or biological effects. Their dependence is thus obtained phenomenologically rather than empirically.

5. The shock waves and their effects

Thermomechanical effects stem from the highly inhomogeneous dose deposition by ions. The ions lose most of their energy in the processes of ionization and excitation of the molecules of the medium. As a result a large number of electrons and holes are produced in the vicinity of the ion's path. These processes happen within 10^{-16} s. The electrons lose their energies in cascades of collisions and thermalize by about $10^{-15} - 10^{-14}$ s. At this time they transfer their energy to the molecules. The energy in the latter is distributed between vibrational and translational degrees of freedom and by $10^{-14} - 10^{-13}$ s the medium in the vicinity of the ion's trajectory becomes very hot. The inelastic thermal spike model predicts the temperature increases to be above 1000 K [10] for carbon ions in liquid water. Consequently, the pressure above 10 GPa is expected within a cylinder of 1 nm around the ion's path. This pressure initiates a cylindrical shock wave that starts at about 10^{-13} s after the ion's passage [11].

The pressure in the front of the shock wave gradually decreases with time. A simplified hydrodynamical treatment [11] predicted the propagation of these waves until 1 ns after the ion's passage. During this time, the wave front propagates for over 90 nm. In reality, the shock waves lose their strength sooner [13], but still their effects are expected at distances over 10 nm even for carbon ions. In relation to the radiation damage, we are interested in two effects. First is the rapid increase of pressure in the wave front with a consequent sharp decrease in the wake of the wave [11]. The second effect is the mass flow transferred by the shock wave.

The pressure on the wavefront is given by [11],

$$P(t) = \frac{2}{\gamma + 1} \rho u_f^2 = \frac{\beta^2}{2(\gamma + 1)} \frac{\sqrt{\epsilon \rho}}{t}, \quad (2)$$

where t is the time after the ion's traverse, $\gamma = C_P/C_V$ for the medium, u_f is the speed of the wave front, $\beta = 0.863$ is a dimensionless constant related to the geometry of the problem (see Ref. [11] for more detail), $\rho = 1 \text{ g cm}^{-3}$ (for liquid water) is the density of the medium, and ϵ is the fraction of the linear energy transfer (LET) that is carried by the shock wave. The radius, R , of the wave front is given by [11]

$$R(t) = \beta \sqrt{t} \left[\frac{\epsilon}{\rho} \right]^{1/4}. \quad (3)$$

From Eqs. (2) and (3) we can obtain the dependence of pressure on the radius of the wave front:

$$P = \frac{\beta^4}{2(\gamma + 1)} \frac{\epsilon}{R^2}. \quad (4)$$

If a biomolecule, such as DNA, appears to be in the vicinity of the ion's path, forces proportional to the above pressure will act on its parts. These forces can be strong enough to break covalent bonds in the backbone of the DNA and thus contribute to the radiation damage. The question of whether the short-time action of such forces is sufficient to cause DNA strand breaks was analyzed in Refs. [13, 14] using a Molecular Dynamics (MD) simulation of a shock wave propagating through a nucleosome. At small values of LET, the shock waves are not sufficiently strong and the radiation damage is due to chemical effects such as interaction of DNA molecules with free or solvated electrons, free radicals, holes, etc. In Ref. [14], it is shown that for the bonds located about 2 nm from the ion's path, the critical value of LET at which the direct bond breaking by the shock wave starts to dominate over chemical effects is 5 keV/nm. Equation (4) tells us that the same (pressure) forces are achieved for the constant ratio of ϵ/R^2 . This allows us to calculate the radius of dominance of the direct damage by shock waves [14]. A LET of about 5 keV/nm is achieved for Ar ions in the vicinity of the Bragg peak.

The value of LET is proportional to the square of the effective charge of the ion. This means that when the radiation damage is assessed for ions heavier than Ar, the direct effect has to be taken into account.

In order to study the transport effects of the shock wave on radiation damage, one should calculate the production of the reactive species such as free radicals and solvated electrons inside the hot cylinder and then calculate their transport by the wave in liquid water. The major anticipated effect will be the “inflation” of the 2-3-nm radius domain, dominated by ballistic electrons, to a cylinder of a radius of 20-30 nm. Damage mechanism predicted in Ref. [25] may be dominant in this region.

6. Conclusions

The main difference of the multiscale approach to the radiation damage from other methods of assessment of radiation damage is the in-depth focusing on physical effects. The main advantages of the multiscale approach follow from its architecture and are its fundamentality and versatility. The approach evaluates the relative contributions and significance of a variety of phenomena; it elucidates a complex multiscale scenario in sufficient detail and has a solid predictive power. It is structurally simple and inclusive, and allows for modifications and extensions by including new effects on different scales and improvements on the way.

The above effects lead to the calculation of primary biological damage as a result of irradiation of tissue with ions. At this time, there are many unknown parameters that enter these calculations, but the survival curves predicting the probability of cell survival can still be obtained [12]. There is a hope that the comparison with a variety of experiments will allow to build a reliable model for the predictive calculation of the RBE. Such a calculation will be based on the analysis of key effects that are parts of the scenario of radiation damage rather than on empiric coefficients taken from completely different scenario of damage with photons.

A new understanding of the scenario related to the shock wave effects seriously questions the validity of empirical approaches of assessment of biological effects. The notion of thermomechanical effects represents a paradigm shift in the understanding of radiation damage due to ions. These effects should be also considered for high-density ion beams, irradiation with intensive laser fields, and other conditions prone to causing high gradients of temperature and pressure on a nanometer scale. These predictions call for more studies, both theoretical and experimental. Further developments of radiation therapy including the use of sensitizers require similar understanding of a multiscale scenario.

Acknowledgments

We are grateful to the support of COST Action MP1002 “Nano-scale insights in ion beam cancer therapy.”

References

- [1] Surdutovich E and Solov'yov A 2012 *J. Phys.: Conf. Ser.* **373** 012001
- [2] Schardt D, Elsässer T and Schulz-Ertner D 2010 *Rev. Mod. Phys.* **82** 383–425
- [3] Kumar A and Sevilla M 2010 *Chem. Rev.* **110** 7002–7023
- [4] Baccarelli I, Gianturco F, Scifoni E, Solov'yov A and Surdutovich E 2010 *Eur. Phys. J. D* **60** 1
- [5] Solov'yov A, Surdutovich E, Scifoni E, Mishustin I and Greiner W 2009 *Phys. Rev.* **E79** 011909
- [6] Nano-ibct: Nanoscale insights into ion beam cancer therapy (nano-ibct) accessed on 01/2013 URL <http://fias.uni-frankfurt.de/nano-ibct/>
- [7] Surdutovich E and Solov'yov A 2009 *Europhys. News* **40/2** 21
- [8] Surdutovich E, Obolensky O, Scifoni E, Pshenichnov I, Mishustin I, Solov'yov A and Greiner W 2009 *Eur. Phys. J. D* **51** 63–71
- [9] Scifoni E, Surdutovich E and Solov'yov A 2010 *Phys. Rev. E* **81** 021903
- [10] Toulemonde M, Surdutovich E and Solov'yov A 2009 *Phys. Rev. E* **80** 031913
- [11] Surdutovich E and Solov'yov A 2010 *Phys. Rev. E* **82** 051915

- [12] Surdutovich E, Gallagher D C and Solov'yov A V 2011 *Phys. Rev. E* **84** 051918
- [13] Yakubovich A V, Surdutovich E and Solov'yov A V 2012 *Nucl. Instr. Meth. B* **279** 135–139
- [14] Surdutovich E, Yakubovich A V and Solov'yov A V 2013 *Sci. Rep.* **3** 1289
- [15] de Vera P, Garcia-Molina R, Abril I and Solov'yov A V 2013 *Phys. Rev. Lett.* **110** in press
- [16] Pimblott S and LaVerne J 2007 *Rad. Phys. Chem.* **76** 1244–1247
- [17] Pimblott S and Siebbeles L 2002 *Nucl. Instr. Meth. B* **194** 237–250
- [18] Pimblott S, LaVerne J and Mozumder A 1996 *J. Phys. Chem* **100** 8595–8606
- [19] Nikjoo H, Uehara S, Emfietzoglou D and Cucinotta F A 2006 *Radiat. Meas.* **41** 1052
- [20] Surdutovich E and Solov'yov A V 2012 *Eur. Phys. J. D* **66** 245
- [21] Bug M, Surdutovich E, Rabus H, Rosenfeld A B and Solov'yov A V 2012 *Eur. Phys. J. D* **66** 291
- [22] Surdutovich E and Solov'yov A V 2012 *Eur. Phys. J. D* **66** 206
- [23] Park Y, Li Z, Cloutier P, Sanche L and Wagner J 2011 *Radiat. Res.* **175** 240–246
- [24] Sanche L 2010 Low-energy electron interaction with dna: Bond dissociation and formation of transient anions, radicals, and radical anions *Radical and radical ion reactivity in nucleic acid chemistry* ed Greenberg M (New York: J. Wiley & Sons, Inc.) p 239
- [25] Smyth M and Kohanoff J 2012 *J. Am. Chem. Soc.* **134** 9122–9125
- [26] Bethe H 1930 *Ann. Phys.* **397** 325–400
- [27] Bloch F 1933 *Z. Phys. A: Hadrons Nucl.* **81** 363–376
- [28] Bloch F 1933 *Ann. Phys.* **408** 285–320
- [29] Abril I, Garcia-Molina R, Denton C, Kyriakou I and Emfietzoglou D 2011 *Radiat. Res.* **175** 247–255
- [30] Pshenichnov I, Mishustin I and Greiner W 2008 *Nucl. Instr. Meth. B* **266** 1094–1098
- [31] Rudd M E, Kim Y K, Madison D H and Gay T 1992 *Rev. Mod. Phys.* **64** 441
- [32] Barkas W H 1963 *Nuclear Research Emulsions I. Techniques and Theory* vol 1 (New York, London: Academic Press)
- [33] Surdutovich E, Scifoni E, and Solov'yov A 2010 *Mutat. Res.* **704** 206–212
- [34] Scifoni E, Surdutovich E and Solov'yov A 2010 *Eur. Phys. J. D* **60** 115
- [35] Tobias F, Durante M, Taucher-Scholz G and Jakob B 2010 *Mutat. Res.* **704** 54–60
- [36] Ward J 1988 *Prog. Nucleic Acid. Res. Mol. biol.* **35** 95–125
- [37] Ward J 1995 *Radiat. Res.* **142** 362–368
- [38] Malyarchuk S, Castore R and Harrison L 2009 *DNA Repair* **8** 1343–1354
- [39] Sage E and Harrison L 2011 *Mutat. Res.* **711** 123–133
- [40] Surdutovich E, Yakubovich A and Solov'yov A 2010 *Eur. Phys. J. D* **60** 101